AD-A211 574

(2)

UNCLASSIFIED

ITY CLASSIFICATION OF THIS PAGE

REPORT DOCUMENTATION PAGE

Form Approved
OMB No 0704-0188

EPORT SECURITY CLASSIFICATION UNCLASSIFIED	1b RESTRICTIVE MARKINGS C. FILE COPY
ECURITY CLASSIFICATION AUTHORITY	3 DISTRIBUTION AVAILABILITY OF REPORT This document has been approved for public release and sale; its distribution is unlimited.
ECLASSIFICATION / DOWNGRADING SCHEDULE	
RFORMING ORGANIZATION REPORT NUMBER(S) ONR-TR- 8	5 MONITORING ORGANIZATION REPORT NUMBER(S)
NAME OF PERFORMING ORGANIZATION Washington State University Department of Chemistry	6b OFFICE SYMBOL (If applicable)
7a NAME OF MONITORING ORGANIZATION Office of Naval Research Chemistry Division	
6c. ADDRESS (City, State, and ZIP Code) Pullman, WA 99164-4630	7b ADDRESS (City, State, and ZIP Code) Arlington, VA 22217
8a. NAME OF FUNDING / SPONSORING ORGANIZATION	8b OFFICE SYMBOL (If applicable)
9 PROCUREMENT INSTRUMENT IDENTIFICATION NUMBER N00014-87-K-0444	
8c. ADDRESS (City, State, and ZIP Code)	10 SOURCE OF FUNDING NUMBERS

PROGRAM ELEMENT NO	PROJECT NO	TASK NO	WORK UNIT ACCESSION NO
		4131031-3	

11. TITLE (Include Security Classification)
Structural Dependence of the Luminescence from Bis(substituted-benzenethiol)(2,9-dimethyl-1,10-phenanthroline)zinc(II) Complexes

12. PERSONAL AUTHOR(S)
K. J. Jordan, W. F. Wacholtz, G. A. Crosby

13a. TYPE OF REPORT	13b. TIME COVERED	14. DATE OF REPORT (Year, Month, Day)	15. PAGE COUNT
Interim Technical	FROM _____ TO _____	89 Aug 15	30

16 SUPPLEMENTARY NOTATION
Submitted for publication in INORGANIC CHEMISTRY

17 COSATI CODES			18. SUBJECT TERMS (Continue on reverse if necessary and identify by block number)
FIELD	GROUP	SUB-GROUP	luminescence, phase transitions, crystals, phenanthroline zinc, benzenethiol decay times, phosphorescence
07	04		

19 ABSTRACT (Continue on reverse if necessary and identify by block number)

Changes in luminescence spectra and lifetimes of crystalline samples of the title compounds at 77 K are correlated with phase changes of the solids. The ease of conversion among phases is a general property of this class of materials. For bis(benzenethiol)-(2,9-dimethyl-1,10-phenanthroline)zinc(II) complete structure determinations were made of both phases. The attendant changes of the optical properties are ascribed to rotation of the planes of the two thiol rings on a single zinc ion from an approximately perpendicular to a nearly face-to-face conformation as the slowly heated crystal undergoes the phase change. The relevance of these results to the problem of charge-separation in solids is discussed.

20 DISTRIBUTION / AVAILABILITY OF ABSTRACT	21 ABSTRACT SECURITY CLASSIFICATION
☒ UNCLASSIFIED/UNLIMITED ☐ SAME AS RPT ☐ DTIC USERS	Unclassified/unlimited
22a NAME OF RESPONSIBLE INDIVIDUAL Parbury Schmidt	22b TELEPHONE (Include Area Code) (202) 696-4409
	22c OFFICE SYMBOL 1113PS

DD Form 1473, JUN 86 — Previous editions are obsolete.

S/N 0102-LF-014-6603

SECURITY CLASSIFICATION OF THIS PAGE
UNCLASSIFIED

89 8 21 123

OFFICE OF NAVAL RESEARCH

Contract N00014-87-K-0444

R & T Code 4131031-3

TECHNICAL REPORT NO. 8

Structural Dependence of the Luminescence from Bis(substituted-benzenethiol)-(2,9-dimethyl-1,10-phenanthroline)zinc(II) Complexes

by

K. J. Jordan, W. F. Wacholtz, and G. A. Crosby

Prepared for Publication

in

Inorganic Chemistry

Washington State University
Department of Chemistry
Pullman, WA 99164-4630

August 15, 1989

Contribution from the Department of Chemistry and Chemical Physics Program,
Washington State University, Pullman, Washington 99164-4630

Structural Dependence of the Luminescence from Bis(substituted-benzenethiol)-(2,9-dimethyl-1,10-phenanthroline)zinc(II) Complexes

K. J. Jordan, W. F. Wacholtz, and G. A. Crosby*

Abstract

Changes in luminescence spectra and lifetimes of crystalline samples of the title compounds at 77 K are correlated with phase changes of the solids. The ease of conversion among phases is a general property of this class of materials. For bis(benzenethiol)(2,9-dimethyl-1,10-phenanthroline)zinc(II) complete structure determinations were made of both phases. The attendant changes of the optical properties are ascribed to rotation of the planes of the two thiol rings on a single zinc ion from an approximately perpendicular to a nearly face-to-face conformation as the slowly heated crystal undergoes the phase change. The relevance of these results to the problem of charge-separation in solids is discussed.

Introduction

Luminescence from zinc complexes has been used extensively in this laboratory to monitor the effects of subtle structural changes upon the relative rates of radiative and radiationless processes in the crystals and solids. Of particular interest is the process of charge separation. Recently we extended our studies to the solid state where thermal barriers to radiationless processes have been observed.[1] In the course of these investigations we have discovered that some of the complexes exhibit at least two crystalline phases and that the attendant luminescence properties are sensitive functions of the phase purity. Moreover, complete conversion to the high temperature phase can be accomplished by heating to temperatures just below the melting point. A detailed crystallographic study of two phases of the $Zn(PhS)_2(2,9\text{-}Me_2\text{-}phen)$[2] complex reveals that the principal structural change that has occurred involves the relative orientation of the phenyl rings of the two coordinated thiols.

Experimental Section

Synthesis. To a solution of zinc acetate dihydrate (0.22 g, 1 mmol) dissolved in 100 mL of hot ethanol a solution of redistilled benzenethiol (0.21 mL, 2.1 mmol in 10 mL ethanol) was added dropwise with stirring. As the second mmol was added, a white precipitate formed. After five minutes of continual stirring 2,9-dimethyl-1,10-phenanthroline (0.21 g, 1 mmol) dissolved in 10 mL of ethanol was added dropwise. The mixture was heated and stirred for a half hour as it gradually turned to a deep yellow solution. It was set aside to cool. After 2-3 days at room temperature crystals were harvested and washed with ethanol. Although the reactions were routinely carried out under N_2, the products did not appear to be air-sensitive. A faint odor of thiol was evident when sample vials were opened, but old samples produced luminescence essentially

indistinguishable from fresh ones. All the compounds reported in this article were synthesized by the same method.

Although $Zn(PhS)_2(2,9\text{-}Me_2\text{-}phen)$ generally produced monoclinic crystals, recrystallization of a sample at room temperature in an open beaker yielded, adventitiously, a crop of large orthorhombic needles. We have been unable to repeat this result, but enough orthorhombic crystals were acquired to carry out the series of measurements reported here on that phase. In the case of $Zn(4\text{-}Cl\text{-}PhS)_2(2,9\text{-}Me_2\text{-}phen)$ two crystal types were obtained simultaneously from the mother liquor and could be separated mechanically. The $Zn(PhS)_2(2,9\text{-}Me_2\text{-}4,7\text{-}Ph_2\text{-}phen)$ molecule was only obtained in the 'low temperature' phase during the initial crystallization process.

Optical Measurements. Emission studies at 77 K were performed in a Pyrex dewar. Crystals were suspended in a thin film of mineral oil that was held by surface tension within a wire loop immersed in liquid N_2. The samples were excited by the 364-nm line from a Coherent 90-5 UV argon ion laser. Typical intensities were 0.3 mW mm^{-2}. The emitted light was dispersed by an Instruments SA HR-640 grating monochromator (1200 lines/mm) and detected with a Hammamatsu R943 photomultiplier. The signal was measured by a Stanford Research Systems SR400 photon counter in either cw or gated mode. All reported spectra were corrected for spectral response of the system by means of a standard tungsten lamp.

For lifetime measurements the cw beam was square-wave modulated with a Conoptics Model 10/380 Electro-optic Modulator driven by a Wavetek 191 Function Generator. The time resolution (100 ns) was limited by the 10-MHz response frequency of the modulator. The curves were fit over 5 decay times for which the baseline was chosen to be at the minimum point. This procedure was necessary because the system does not provide 100% depth of modulation.

DSC Measurements. The differential scanning calorimetric measurement was performed on a Perkin-Elmer DSC7 instrument. Orthorhombic $Zn(PhS)_2(2,9\text{-}Me_2\text{-}phen)$ crystals (14.3 mg) were ground to a fine powder and sealed in an aluminum sample cup. The reference was a similar can sealed with air. A scan rate of $10^{o}C$ per minute was employed. A 77 K emission spectrum confirmed that grinding the crystals did not induce a phase change.

Crystallographic Data Collection and Structure Determinations. X-ray diffraction data collections were performed on a Syntex $P2_1$ diffractometer upgraded to Nicolet P3F speficications, and the structures were solved by employing direct methods with the version 5.1 SHELXTL structure solution package.[3] Data for both forms of the complex were collected by means of graphite monochromated Mo Ka radiation.[4] Accurate unit cell parameters were obtained through centering of 25 reflections with 2θ values between 29^{o} and 36^{o} for the monoclinic form and 20^{o} and 26^{o} for the orthorhombic form of the complex. Empirical absorption corrections were made assuming an ellipsoidal crystal for both the monoclinic and orthorhombic forms of the complex. Pertinent crystallogrphic parameters are included in Table I with a more complete table of crystallographic parameters available through supplementary material.

For both forms of the complex direct methods revealed the zinc atoms. Subsequent difference maps revealed the positions of all other non-hydrogen atoms. Hydrogen atoms were fixed at calculated positions (r_{C-H} = 0.96 Å). The thermal parameters were anisotropic on all non-hydrogen atoms for the monoclinic form of the complex. For the orthorhombic form the thermal parameters were anisotropic on all non-carbon, non-hydrogen atoms and on selected carbon atoms expected to exhibit the most thermal motion (Table IV). The thermal parameters for all hydrogen atoms were fixed at approximately 1.2 times the corresponding

heavier atom thermal parameter. Selected bond lengths and angles are given in Tables II and III, respectively. Atomic coordinates and thermal parameters are given in Table IV. The standard ACS X-ray data collection parameters long form, complete bond lengths and angles, complete listings of hydrogen atom positions and anisotropic thermal parameters as well as a tabulation of the $|F_o|$ and $|F_c|$ values have been deposited.

Results

Phase Changes. The incidence of a phase transition could be monitored visually in a melting point apparatus. As the temperature of the low-temperature phase (orthorhombic) was raised, a subtle, but definite, cracking could be observed over a narrow range. No other physical changes were evident until the crystals approached their melting points when a decided darkening of the color set in. Once taken through the phase change, by heating, the crystals remained in the high temperature metastable phase upon cooling. Holding the temperature for several days just below the transition temperature did not regenerate the second phase. The phase transition temperatures as determined by cracking are given in Table V along with the melting points.

A differential scanning calorimetric measurement was performed on a powdered sample of $Zn(PhS)_2(2,9\text{-}Me_2\text{-}phen)$ in the orthorhombic phase. The onset of an endothermic transition was detected by DSC at 140°C and finally peaked at 144°C.

Structure Description. Both forms of the complex $Zn(PhS)_2(2,9\text{-}Me_2\text{-}phen)$ pack as discrete molecules with a distorted tetrahedral geometry around the central zinc atom (Figure 1). The zinc-sulfur bond lengths are 2.255(2) Å for $Zn\text{-}S_1$ and $Zn\text{-}S_2$ in the monoclinic form and 2.257(4) Å and 2.270(3) Å in the orthorhombic form, respectively. For a regular tetrahedron, bond angles would be expected to be 109.5°; however, in both forms of the complex the bond angles

are notably different from this ideal value (Table III). This is expected due to the nature of the N,N-heterocycle and the possibility of a large degree of flexibility in the thiol ligand. The 2,9-Me_2-phen ligand defines a plane in both forms of the complex and exhibits a rocking motion in that plane as observed from the thermal ellipsoids shown in Figure 1. It appears that the methyl substituents effectively lock in the ligand so that motion perpendicular to the plane of the ligand is significantly reduced when compared to other planar N,N-heterocyclic ligands that lack methyl substituents.

The benzenethiol ligands adopt a different orientation with respect to each other depending on the crystal form. In the monoclinic phase they are more face to face and are in fact symmetrically related through an inversion operation. In the orthorhombic form the planes of the benzene rings are more perpendicular to each other and are not related by symmetry. This understandably affects the bond angles around the sulfur atoms in these two complexes (Table III) and might account for the observed photophysical differences (vide infra). There appear to be no abnormally long carbon-nitrogen, carbon-carbon, or carbon-sulfur bonds in either of the two crystalline forms.

The planes of one substituted-phenanthroline ligand overlap with a substituted-phenanthroline ligand on an adjacent molecule to produce a pseudo-dimer (Figure 2). The overlap, however, is not especially good and has been observed to be much better in other multinuclear zinc dithiol complexes.[5] The distance separating the two ligands within the pseudo-dimer is 3.36(1) Å and 3.45(1) Å for the monoclinic and orthorhombic forms, respectively. Both phases of the complex appear to exhibit their pseudo-dimeric packing with benzenethiol ligands located between the pseudo-dimers (Figure 3); however, there is no significant overlap of the thiol ligands with the phenanthroline moieties of the pseudo-dimer units. We note that this packing does not appear to generate a

one-dimensional linear chain system in either form, since only interactions within the pseudo-dimers are possible.

Spectral Data. Essential emission spectra are presented in Figures 4 - 6. In Figure 4 the spectrum of the orthorhombic phase of $Zn(PhS)_2(2,9\text{-}Me_2\text{-}phen)$ is seen to peak at 660 nm, whereas that of the monoclinic phase maximizes at 565 nm. Although the plotted spectra are normalized, the latter emission is significantly (5x) brighter than the former. Moreover, a hint of structure appears on the high energy side of the spectrum of the monoclinic crystals. This feature is enhanced when the sample is cooled to 4.5 K (not shown) but never appears in the emission from the orthorhombic material. (There is also a very weak long-lived structured π-π^* phosphorescence in the 77 K spectrum of the monoclinic phase that obviously arises from the $2,9\text{-}Me_2$-phen ligand.) In the spectrum from the orthorhombic phase at 4.5 K a shoulder becomes apparent at 530 nm. It is important to note that the optical properties of the monoclinic phase are the same irrespective of whether the sample was obtained directly from the original preparation or from maintaining an orthorhombic crystal for several minutes at 150°C, i.e., about 10°C above the transition temperature.

In Figure 5 spectra of $Zn(4\text{-}Cl\text{-}PhS)_2(2,9\text{-}Me_2\text{-}phen)$ are displayed. The emission from the low-temperature phase maximizes at 590 nm and that of the second phase at 550 nm. The latter emission is brighter (3x) than the former and can be generated either by holding the low-temperature phase at 193°C for three minutes or using the translucent crystals that were originally separated mechanically from the mother liquor.

In Figure 6 the emission data for $Zn(PhS)_2(2,9\text{-}Me_2\text{-}4,7\text{-}Ph_2\text{-}phen)$ are shown. The structured emission of the first phase is replaced by a diffuse band that is considerably red-shifted from the former and peaks at 650 nm. The latter spectrum was obtained by maintaining the originally obtained crystals at 132°C

for three minutes. This temperature is above the phase transition temperature but well below the melting point of the substance.

Although the decay times of the emissions are often non-exponential, it is significant that they, too, are independent of the way the phase was produced. Decay curves from crystals of a high temperature phase obtained directly upon crystallization are identical to those obtained from this same phase when it was generated by annealing the other phase, as previously described.

Discussion

The discovery of multiple crystalline phases of members of this class of complexes and the subsequent determinations of the two crystal structures of $Zn(PhS)_2(2,9\text{-}Me_2\text{-}phen)$ are significant advances in our goal to understand the factors determining energy conversions among states in these substances. In particular, the origin of the previously reported thermal barriers to energy migration between π-π^* and ligand-ligand charge-transfer (LLCT) states is a major goal.[1] As the spectra clearly reveal, the dependence of the emission parameters on solid state structure is significant (vide infra). Although changes in lifetime are certainly expected since decay times are generally observed to be very sensitive to small perturbations of the structure, the large shifts in the emission energies were unexpected. Shifts of 1200 cm^{-1} of peak maxima subsequent to a thermally-induced phase change indicate major perturbations of the energy levels of the molecules.

Some correlations among the various sets of data are obvious. In general, at 77 K the low-temperature phases display shorter, often non-exponential, decay times and the spectra are much weaker than those from the high temperature phases, which also yield decays at 77 K that are more nearly exponential. We conjecture that the low-temperature phase possesses more thermal motion in the crystal, particularly as the phase transition temperature is approached, and

that this leads to enhanced radiationless coupling and lower emission quantum yields. There may also be more than one low-temperature phase in some cases. In general, the emission band of the high temperature phase is blue-shifted from that emanating from the other phase, but the $Zn(PhS)_2(2,9\text{-}Me_2\text{-}4,7\text{-}Ph_2\text{-}phen)$ complex supplies the counter example. There appears to be a correlation between the ease of producing both crystalline forms simultaneously during preparation or recrystallization---the closer the phase-transition temperature is to the melting point, the better the chances for harvesting both types of crystals. This seems kinetically and thermodynamically reasonable.

To search for structural factor(s) dictating the large energy shifts of the emissions between the two observed phases, we appeal to the detailed crystallographic data on $Zn(PhS)_2(2,9\text{-}Me_2\text{-}phen)$. As Tables 2 and 3 show, only minor changes in bond lengths and angles occur when the crystallographic morphology changes. Moreover, both forms of the complexes exhibit a pseudo-dimeric packing in the crystals and the ring overlap with adjacent molecules is not especially good. Thus, we find no compelling reason to attribute the large spectral shift of the emission to intermolecular factors. Indeed, the only salient structural difference between the two forms appears to be the relative orientation of the thiol rings coordinated to the same zinc ion. In the monoclinic (high-temperature) phase the rings approach a face-to-face orientation and are, in fact, related by symmetry, but in the orthorhombic phase the two ring planes are almost perpendicular.

If one accepts the notion that the energy shift of the emission can be ascribed to the change in the orientation of the thiol rings, then the orbital natures of the excited states from which emission occurs must be considered. Previously the broad, diffuse bands from these complexes have been assigned to LLCT transitions.[6,7] Excitation of the complex to this kind of configuration transfers negative charge from the HOMO on the thiols to the LUMO on the

phenanthroline ligand. Face-to-face orientation of the thiol rings should lower the ground state and therefore raise the energy of the transition, precisely what is observed. This argument ignores the energy involved in twisting the plane of the one thiol ring with respect to the plane defined by the S, Zn, and S-linked carbon atom of the thiol ring. For aromatic thiols in the gas phase this energy has been determined to be ca. 300 cm^{-1},[8,9] but the difference in twisting energy between a H-S and Zn-S linkage and the phenyl ring is unknown. If the ground state energy of the twisted ring conformation is <u>raised</u> with respect to the face-to-face arrangement, as the gas phase measurements on the ligand imply, then the emission from this form should also be red shifted, as observed. Thus, we tentatively ascribe the observed blue-shift of the emission spectrum of $Zn(PhS)_2(2,9\text{-}Me_2\text{-}phen)$ to a stabilization of the ground electronic state of the complex due to the dispersion forces between the two face-to-face thiol rings and a possible barrier to twisting the thiol ring with respect to the plane of the Zn-S-C linkage. For the complex that displays a red-shift of the emission when it is converted to the high-temperature form, then one would predict a <u>destabilization</u> of the ground state in the latter phase. The relative thermodynamic stabilities of the phases would be governed by both energetic and entropic terms, however.

The results from these studies shed light on several problems we have encountered during our investigations of these and analogous closed-shell complexes. In glass matrices we have never been able to obtain strictly exponential decays and we are convinced that multiple conformations of the complexes lie at the root of the problem. Evidently, the lack of any strong electronic factors dictating the geometry allows several conformations of comparable energy to be realized in a glass matrix and produce both multiple decays and LCCT bands.

The current results also explain why thermally accessible barriers between π-π^* and LLCT excited states are difficult to design into the complexes by making subtle chemical substitutions on the chelated rings. Barriers only appear when the states separating them are nearly isoenergetic, i.e., lie within a few hundred wavenumbers.[10] Since conformational changes in the crystal lead to energy shifts that exceed this limit, then the somewhat capricious occurrence of thermally accessible barriers becomes understandable.

Finally, we comment on the relevance of these results to the fundamental process of charge separation in molecules and solids. If thermally surmounting barriers between π-π^* and LLCT excited states in these compounds does indeed represent irreversible conversion to a charge-separated configuration, then the sensitive dependence of the barrier height and, thereby, the rate of the separation process, on the conformation of the complex could explain how very minor changes in structure can lead to enormous changes in rates.

Acknowledgment. This research was supported in part by the Office of Naval Research and the Department of Energy under Grant No. DE-FG06-87ER13809. Such support does not constitute an endorsement by DOE of the views expressed in this article.

Supplementary Material Available: Tables of X-ray data collection parameters (Table S1), bond lengths for the monoclinic and orthorhombic forms (Table S2), bond angles for the monoclinic and orthorhombic forms (Table S3), anisotropic thermal parameters for the monoclinic and orthorhombic forms (Table S4), hydrogen atom positions and isotropic thermal parameters for the monoclinic and orthorhombic forms (Table S5)(5 pages); stereopacking diagrams of bis(benzenethiol)(2,9-dimethyl-1,10-phenanthroline)zinc(II)(Figure S1)(1 page). Ordering information is given on any current masthead page.

References

(1) Highland, R. G.; Crosby, G. A. Chem. Phys. Lett. **1985**, 119, 454.

(2) Compounds are identified in Table V.

(3) Sheldrick, G. "SHELXTL", Nicolet Analytical Instruments, Madison, WI, 1985.

(4) Campana, C. F; Shepard, D. F.; Litchman, W. M. Inorg. Chem. **1981**, 20, 4039.

(5) Wacholtz, W. F.; Jordan, K. J.; Crosby, G. A. Submitted for publication.

(6) Koester, V. J. Chem. Phys. Lett. **1975**, 32, 575.

(7) Crosby, G. A.; Highland, R. G.; Truesdell, K. A. Coord. Chem. Rev. **1985**, 64, 41.

(8) Schaefer, T; Parr, W. J. E. Can. J. Chem. **1977**, 55, 552.

(9) Larsen, N. W.; Nicolaisen, F. M. J. Mol. Structure **1974**, 22, 29.

(10) Van Houten, J.; Watts, R. J. J. Am. Chem. Soc. **1976**, 98, 4853.

FIGURE CAPTIONS

Figure 1. Thermal ellipsoid plots of the structure of $Zn(PhS)_2(2,9\text{-}Me_2\text{-}phen)$: monoclinic phase (top); orthornombic phase (bottom).

Figure 2. Projection diagrams of $Zn(PhS)_2(2,9\text{-}Me_2\text{-}phen)$ showing overlaps of N,N-heterocyclic rings of adjacent molecules.

Figure 3. Stereopacking diagrams of $Zn(PhS)_2(2,9\text{-}Me_2\text{-}phen)$: monoclinic phase (top); orthornombic phase (bottom).

Figure 4. Emission spectra of $Zn(PhS)_2(2,9\text{-}Me_2\text{-}phen)$ at 77 K: A, monoclinic phase; B, orthorhombic phase.

Figure 5. Emission spectra of $Zn(4\text{-}Cl\text{-}PhS)_2(2,9\text{-}Me_2\text{-}phen)$ at 77 K: A, clear yellow crystals; B, clear yellow crystals after undergoing a phase transition. This spectrum is identical to that obtained from the originally-obtained translucent yellow crystals.

Figure 6. Emission spectra of $Zn(PhS)_2(2,9\text{-}Me_2\text{-}4,7\text{-}Ph_2\text{-}phen)$ at 77 K: A, original crystals; B, crystals after annealing at 132°C (3 min).

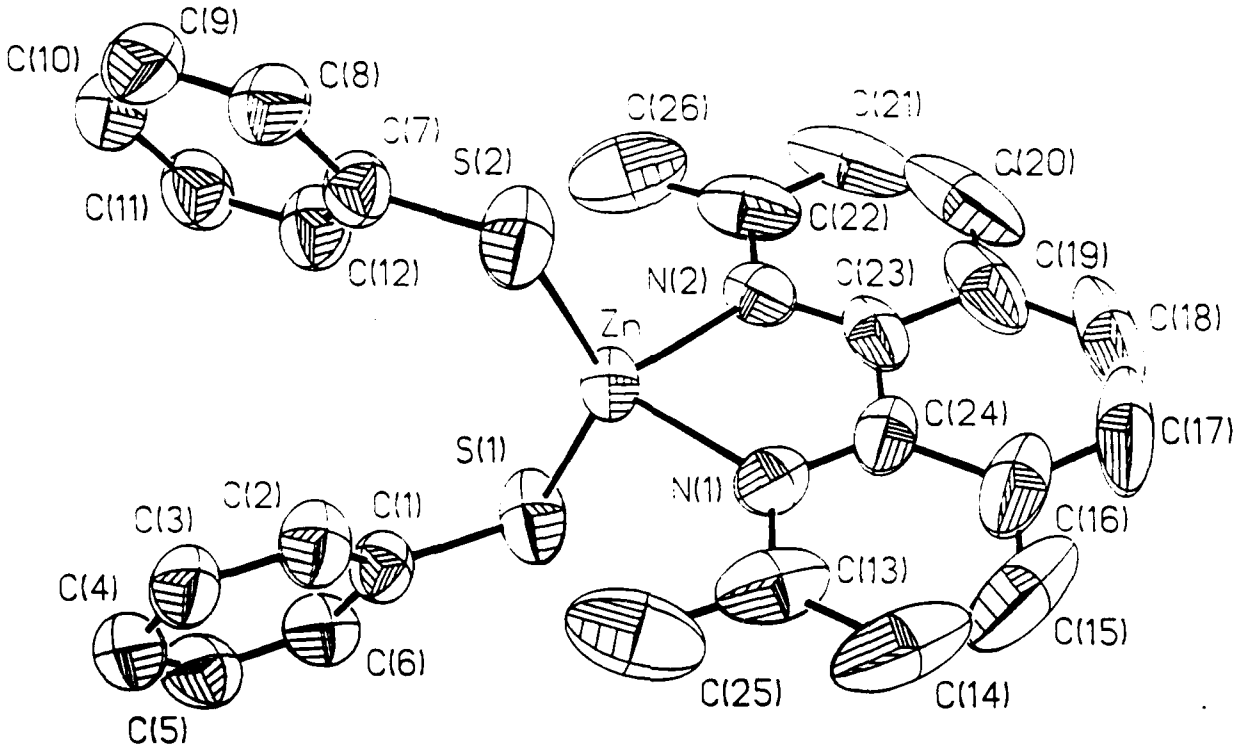
C(9)
C(10)
C(8)
C(7)
S(2)
C(26)
C(21)
C(11)
C(22)
C(20)
C(12)
N(2)
C(23)
C(19)
Zn
C(18)
C(24)
C(17)
S(1)
N(1)
C(2)
C(1)
C(16)
C(3)
C(13)
C(4)
C(15)
C(6)
C(25)
C(14)
C(5)

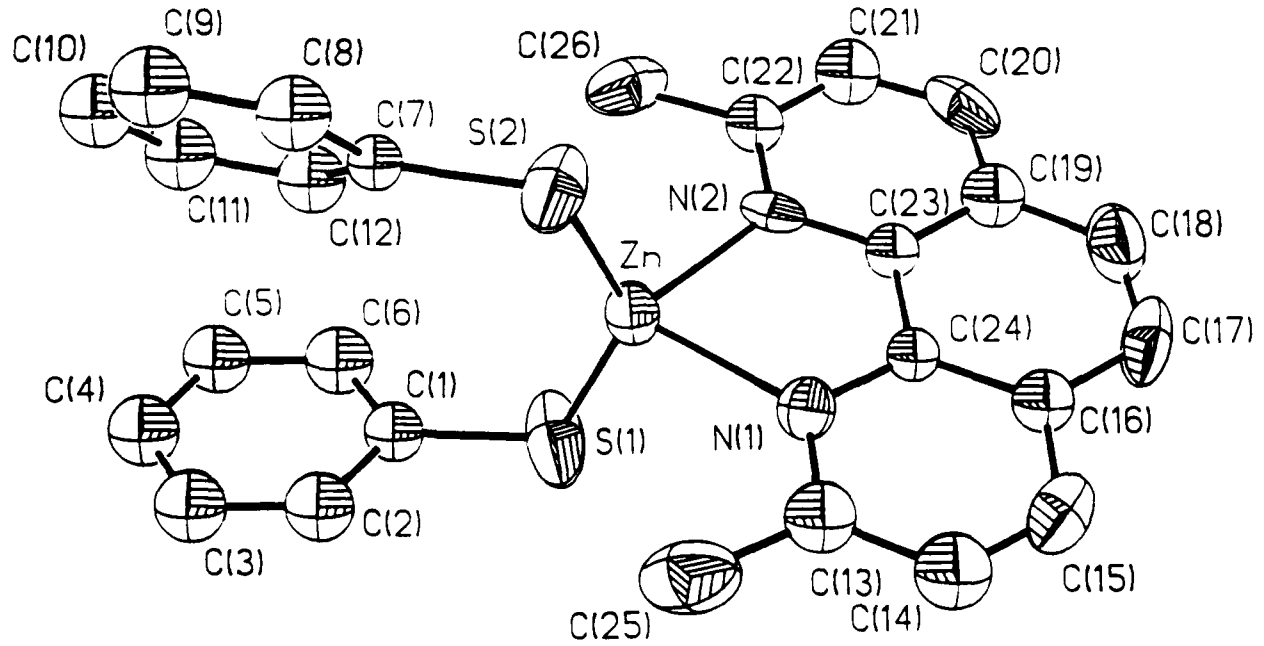
C(10)
C(9)
C(8)
C(26)
C(21)
C(22)
C(20)
C(7)
S(2)
C(11)
C(19)
N(2)
C(23)
C(12)
C(18)
Zn
C(5)
C(6)
C(24)
C(17)
C(4)
C(1)
C(16)
S(1)
N(1)
C(2)
C(3)
C(13)
C(15)
C(25)
C(14)

Figure 1

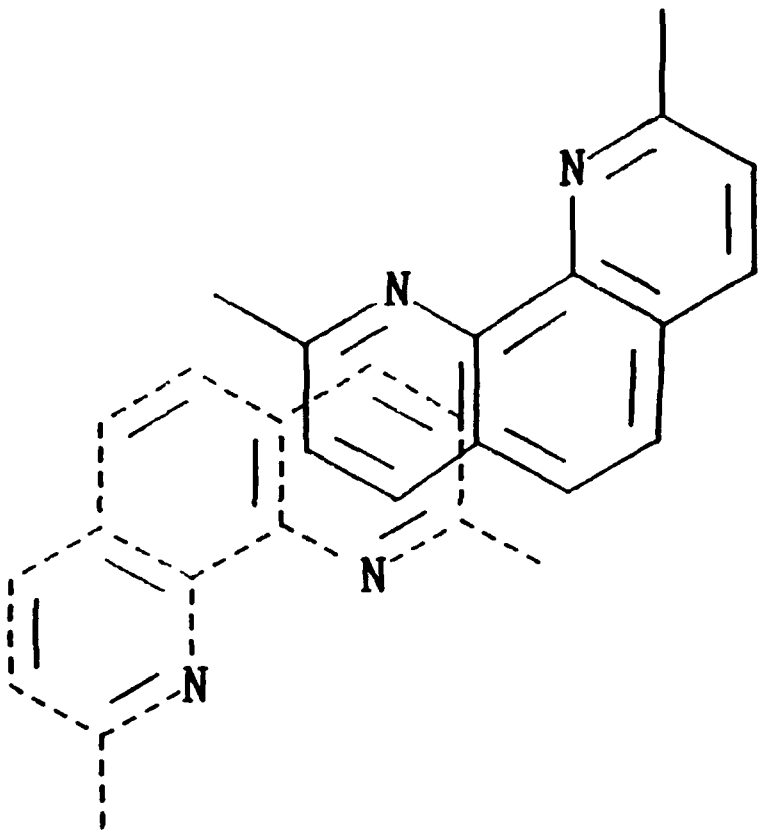

Monoclinic

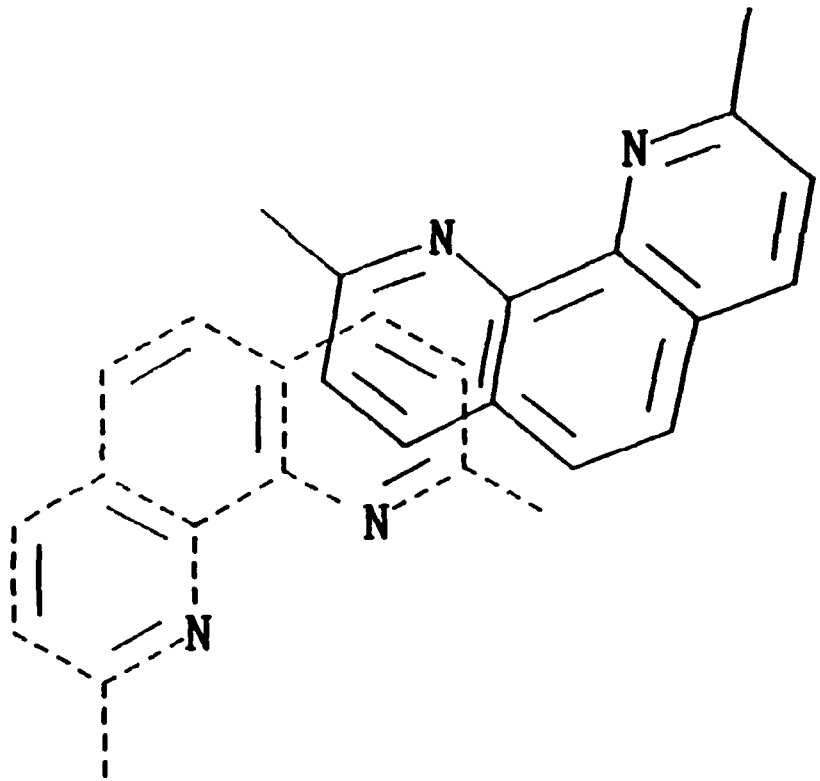

Orthorhombic

Figure 2

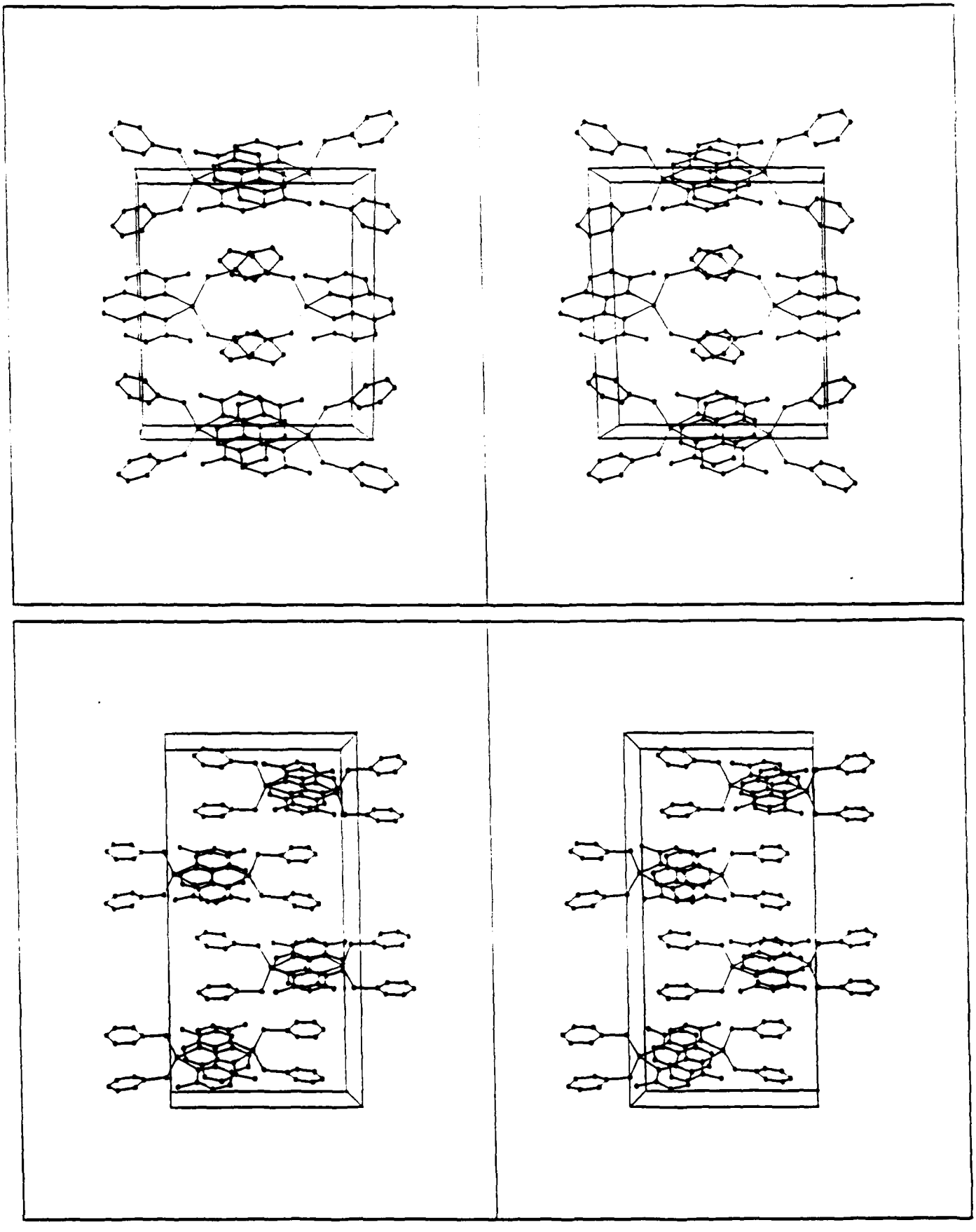

Figure 3

Figure 4

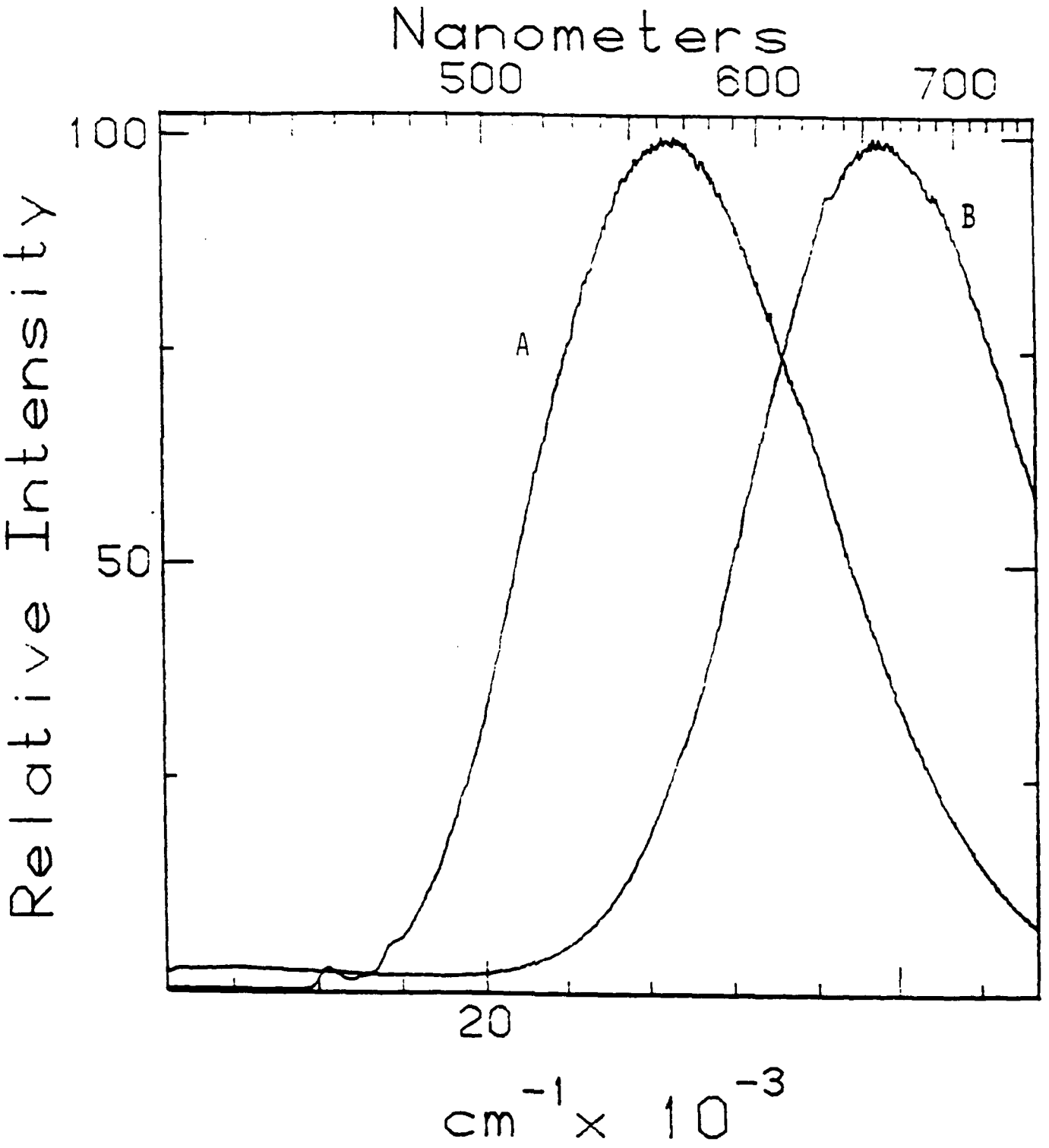
Nanometers
500
600
700
100
50
Relative Intensity
A
B
20
cm⁻¹ × 10⁻³

Figure 5

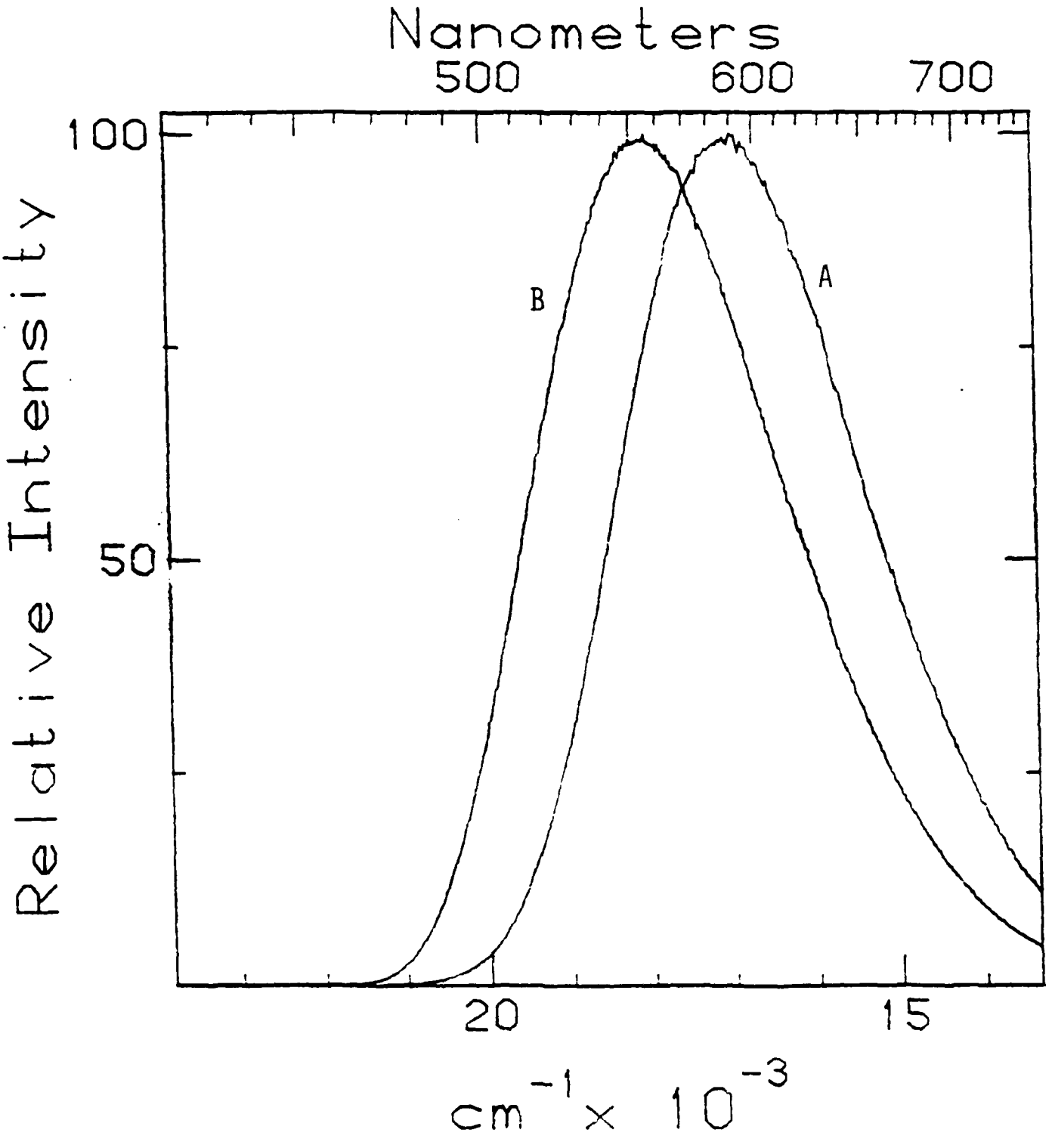
Nanometers
500
600
700
100
50
Relative Intensity
B
A
20
15
cm⁻¹ x 10⁻³

Figure 6

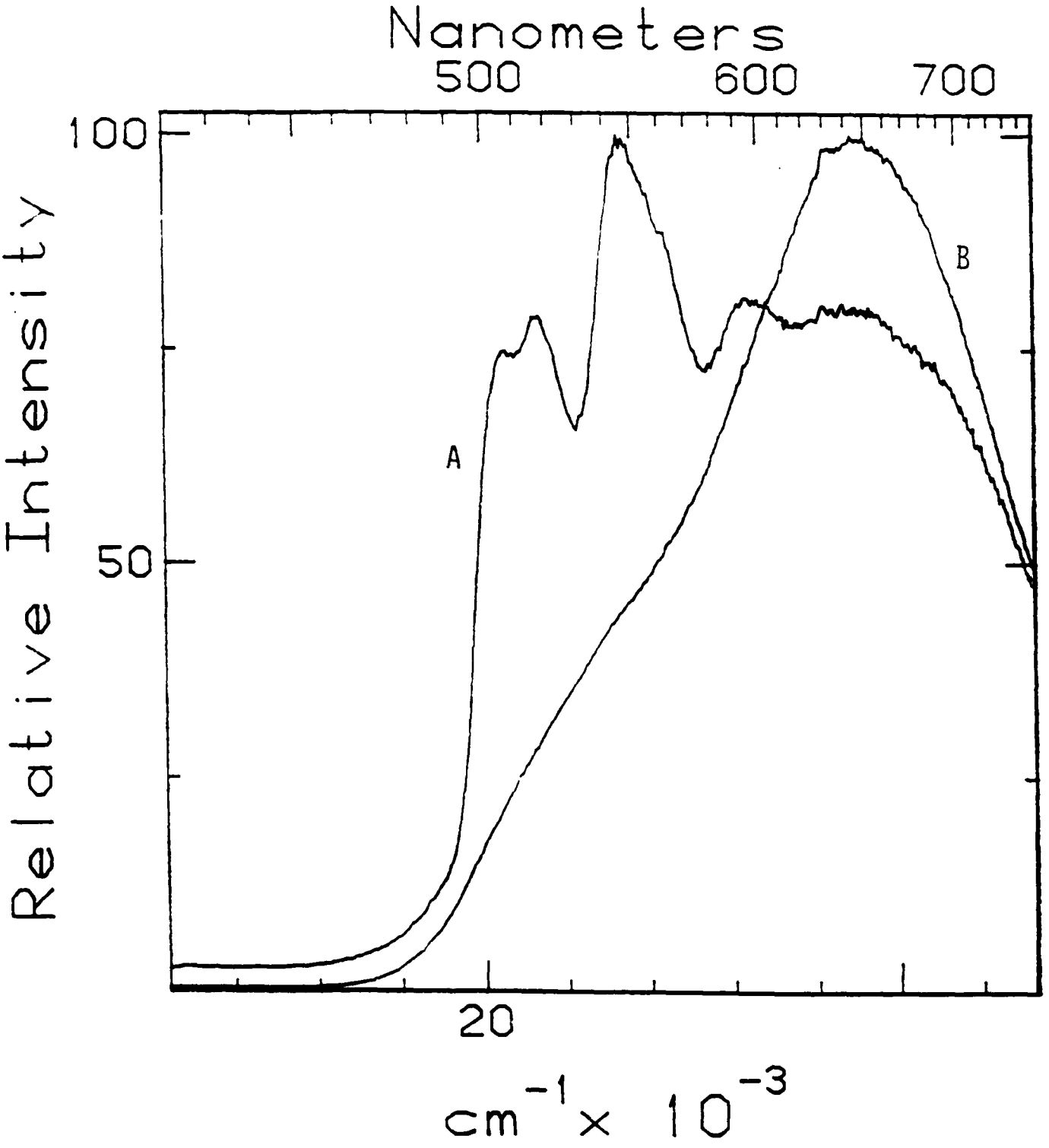
Nanometers
500
600
700
100
50
Relative Intensity
A
B
20
cm⁻¹ x 10⁻³

Table I. Crystallographic Data for the Monoclinic and Orthorhombic Crystals of $Zn(Ph\text{-}S)_2(2,9\text{-}Me_2phen)$

	monoclinic	orthorhombic
chemical formula	$ZnC_{26}H_{22}N_2S_2$	$ZnC_{26}H_{22}N_2S_2$
formula weight	491.69	491.69
space group	C 2/c	Pbca
a, Å	15.418 (3)	27.296 (8)
b, Å	13.154 (2)	13.941 (3)
c, Å	11.556 (2)	12.139 (5)
β, deg	101.46 (1)	
V, Å^3	2297.1 (6)	4619 (2)
Z	4	8
T	ambient	ambient
λ, Å	0.71069	0.71069
ρ_{calcd}, g-cm^{-3}	1.42	1.41
μ, cm^{-1}	12.9	12.8
$R(F_o)$	0.0539	0.0864
$R_w(F_o)$	0.0493	0.0490

Table II. Selected Interatomic Distances (Å) for the Monoclinic and Orthorhombic Forms of $Zn(Ph\text{-}S)_2(2,9\text{-}Me_2phen)$

	monoclinic	orthorhombic
Zn-S(1)	2.255 (2)	2.257 (4)
Zn-S(2)	2.255 (2)	2.270 (3)
Zn-N(1)	2.086 (4)	2.128 (7)
Zn-N(2)	2.086 (4)	2.114 (7)
S(1)-C(1)	1.758 (4)	1.768 (10)
S(2)-C(7)	1.758 (4)	1.777 (9)
C(1)-C(2)	1.391 (7)	1.362 (15)
C(1)-C(6)	1.388 (7)	1.398 (15)
C(7)-C(8)	1.391 (7)	1.395 (14)
C(7)-C(12)	1.388 (7)	1.381 (14)

Table III. Selected Interatomic Angles (deg) for the Monoclinic and Orthorhombic Forms of $Zn(Ph\text{-}S)_2(2,9\text{-}Me_2phen)$

	monoclinic	orthorhombic
S(1)-Zn-S(2)	134.5 (1)	138.1 (1)
S(1)-Zn-N(1)	106.7 (1)	106.2 (2)
S(2)-Zn-N(1)	107.7 (1)	103.9 (2)
S(1)-Zn-N(2)	107.7 (1)	105.3 (2)
S(2)-Zn-N(2)	106.7 (1)	108.6 (2)
N(1)-Zn-N(2)	80.2 (2)	79.0 (3)
Zn-S(1)-C(1)	109.8 (2)	110.4 (4)
Zn-S(2)-C(2)	109.8 (2)	111.9 (3)
C(2)-C(1)-S(1)	124.5 (4)	120.6 (8)
C(6)-C(1)-S(1)	117.5 (4)	121.8 (8)
C(8)-C(7)-S(2)	124.5 (4)	117.9 (7)
C(12)-C(7)-S(2)	117.5 (4)	124.3 (7)

Table IV. Atomic Positional Parameters (x 10^4) for the Monoclinic and Orthorhombic Forms of Zn(Ph-S)$_2$(2,9-Me$_2$phen)

	monoclinic				orthorhombic			
	x	*y*	*z*	*U*[a]	*x*	*y*	*z*	*U*[a]
Zn	0	2617 (1)	2500	49 (1) *	1291 (1)	4609 (1)	3496 (1)	44 (1) *
S(1)	1108 (1)	1954 (1)	1725 (1)	77 (1) *	1928 (1)	5162 (2)	4500 (3)	87 (2) *
S(2)[b]					705 (1)	5209 (2)	2364 (3)	61 (1) *
N(1)[b]					1553 (3)	3377 (5)	2646 (7)	39 (3) *
N(2)	-518 (2)	3830 (3)	1417 (3)	55 (1) *	980 (3)	3498 (5)	4453 (6)	36 (3) *
C(1)	1381 (3)	739 (3)	2320 (4)	57 (2) *	1913 (4)	6429 (7)	4566 (9)	45 (3)
C(2)	1034 (3)	308 (4)	3229 (4)	69 (2) *	2110 (4)	6969 (8)	3742 (9)	57 (4)
C(3)	1269 (3)	-667 (4)	3627 (5)	72 (2) *	2125 (4)	7967 (8)	3816 (10)	64 (4)
C(4)	1851 (4)	-1229 (4)	3139 (5)	78 (2) *	1937 (4)	8418 (8)	4710 (10)	64 (4)
C(5)	2208 (4)	-808 (4)	2251 (5)	80 (2) *	1741 (4)	7903 (7)	5551 (9)	61 (4)
C(6)	1971 (3)	165 (4)	1829 (4)	65 (2) *	1733 (4)	6903 (7)	5497 (10)	61 (4)
C(7)[b]					633 (3)	6468 (6)	2531 (8)	31 (3)
C(8)[b]					391 (3)	6973 (7)	1700 (9)	53 (3)
C(9)[b]					317 (4)	7948 (8)	1823 (9)	61 (4)
C(10)[b]					477 (3)	8433 (7)	2734 (9)	55 (3)
C(11)[b]					706 (3)	7944 (7)	3581 (9)	57 (3)
C(12)[b]					781 (3)	6973 (7)	3451 (9)	50 (3)
C(13)[b]					1841 (4)	3340 (7)	1751 (10)	52 (3)
C(14)[b]					1970 (3)	2448 (8)	1307 (8)	58 (3)
C(15)[b]					1823 (3)	1633 (7)	1774 (8)	51 (4) *
C(16)[b]					1522 (3)	1633 (7)	2709 (8)	43 (3)
C(17)[b]					1353 (4)	782 (7)	3249 (9)	62 (5) *
C(18)	-266 (6)	6589 (4)	1998 (11)	154 (9) *	1059 (4)	876 (8)	4154 (10)	68 (6) *
C(19)	-553 (5)	5676 (4)	1379 (8)	102 (3) *	920 (4)	1766 (7)	4626 (9)	48 (3)
C(20)	-1095 (6)	5603 (7)	273 (10)	136 (5) *	634 (3)	1894 (7)	5555 (8)	58 (5) *
C(21)	-1350 (5)	4682 (8)	-231 (7)	123 (4) *	526 (4)	2789 (8)	5918 (9)	57 (4)
C(22)	-1053 (4)	3785 (5)	352 (5)	80 (3) *	699 (4)	3585 (7)	5338 (8)	42 (3)
C(23)	-284 (3)	4738 (3)	1923 (4)	66 (2) *	1092 (3)	2605 (8)	4079 (8)	35 (3)
C(24)[b]					1396 (3)	2539 (6)	3121 (7)	32 (3)
C(25)[b]					1999 (4)	4277 (8)	1305 (10)	78 (6) *
C(26)	-1277 (4)	2777 (5)	-148 (5)	113 (3) *	584 (4)	4587 (8)	5736 (8)	67 (5) *

[a] Isotropic thermal parameters (Å^2 x 10^3) with anisotropic atoms marked with an asterisk. Equivalent isotropic *U* defined as one-third of the trace of the orthogonalized U_{ij} tensor.

[b] Atoms generated by an inversion symmetry operation.

Table V. Phase Change Temperatures, Melting Points, and Decay Times

Compound[a]	Phase Change, ^{o}C[b]	m.p, ^{o}C	τ (77^{o}C),[c] μs
$Zn(PhS)_2(2,9\text{-}Me_2\text{-}phen)$			
monoclinic	-	217-218	230[d]
orthornombic	136-143	217-218	<0.1, 0.3, 1.3[d]
$Zn(4\text{-}Cl\text{-}PhS)_2(2,9\text{-}Me_2\text{-}phen)$			
translucent yellow crystals	-	224-225	5[d]
clear yellow crystals	185-187	224-225	3.9, 28[d]
$Zn(PhS)_2$-$(2,9\text{-}Me_2\text{-}4,7\text{-}Ph_2\text{-}phen)$			
high-temperature phase		181-183	15, >1000[e]
low-temperature phase	125-130	181-183	7, 99[e]
$Zn(F_5\text{-}PhS)(2,9\text{-}Me_2\text{-}phen)$	180-182	206-207	

[a] $Zn(PhS)_2(2,9\text{-}Me_2\text{-}phen)$ = bis(benzenethiol)(2,9-dimethyl-1,10-phenanthroline)-zinc(II); $Zn(4\text{-}Cl\text{-}PhS)_2(2,9\text{-}Me_2\text{-}phen)$ = bis(4-chlorobenzenethiol)(2,9-dimethyl-1,10-phenanthroline)zinc(II); $Zn(PhS)_2(2,9\text{-}Me_2\text{-}4,7\text{-}Ph_2\text{-}phen)$ = bis-(benzenethiol)(2,9-dimethyl-4,7-diphenyl-1,10-phenanthroline)zinc(II); $Zn(F_5\text{-}PhS)(2,9\text{-}Me_2\text{-}phen)$ = bis(pentafluorobenzenethiol)(2,9-dimethyl-1,10-phenanthroline)zinc(II).

[b] estimated from observing cracking in melting point apparatus.

[c] λ_{ex} = 363.8 nm.

[d] measured at 600 nm.

[e] measured at 650 nm, dominant components.

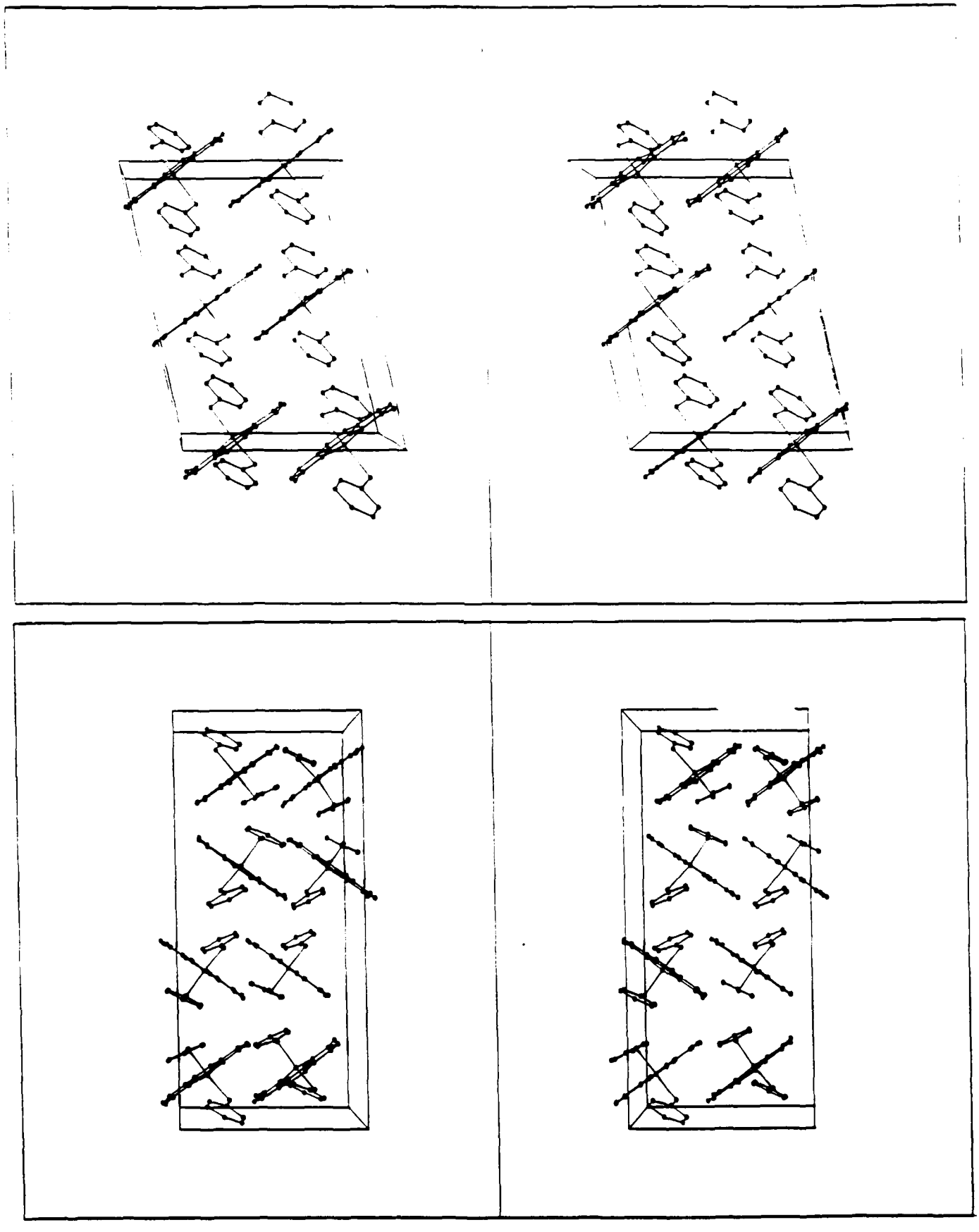

Figure S1

Table S-I. X-ray Data Collection Parameters

	monoclinic	orthorhombic
empirical formula	$ZnC_{26}H_{22}N_2S_2$	$ZnC_{26}H_{22}N_2S_2$
molecular weight, g/mole	491.69	491.69
crystal class	monoclinic	orthorhombic
space group	C2/c	Pbca
orientation reflections		
number, 2θ, deg	25, 29 < 2θ < 36	25, 20 < 2θ < 26
a, Å	15.418 (3)	27.296 (8)
b, Å	13.154 (2)	13.941 (3)
c, Å	11.556 (2)	12.139 (5)
α, deg	90.0	90.0
β, deg	101.46 (1)	90.0
γ, deg	90.0	90.0
V, Å^3	2297.1 (6)	4619 (2)
Z	4	8
ρ_{calcd}, g-cm^{-3}	1.42	1.41
crystal size, mm	0.58 x 0.20 x 0.15	0.43 x 0.14 x 0.15
μ, cm^{-1}	12.9	12.8
diffractometer system	Upgraded Syntex $P2_1$	Upgraded Syntex $P2_1$
radiation	Mo Kα (.71069) with graphite monochrometer	
absorption correction	ellipsoidal	ellipsoidal
transmission range	0.849 < x < 0.944	0.729 < x < 0.953
temperature	ambient	ambient
scan method	ω	ω
data collection range	3 < 2θ < 45	3 < 2θ < 45
scan speeds, deg/min	4 < x < 29.3	4 < x < 29.3
no. of unique data; total number with $F_o^2 > 3\sigma(F_o^2)^2$	2118; 1559	3023; 1706
total parameters refined	144	186
R [a]	0.0539	0.0864
R_w [b]	0.0493	0.0490
g	0.0004	0.0001
goodness of fit	1.348	1.576
|Δ/σ| (min)	0.002	0.016
|Δ/σ| (max)	0.012	0.072
largest peak on final difference map	0.498	0.666

[a] $R = \dfrac{\Sigma \, ||F_o| - |F_c||}{\Sigma \, |F_o|}$

[b] $R_w = \left[\dfrac{\Sigma \, (|F_o| - |F_c|)^2}{\Sigma \, |F_o|^2} \right]^{1/2}$ with $w = \dfrac{1}{[\sigma^2(F) + g(F)^2]}$

Table S-II. Bond Lengths (Å) for the Monoclinic and Orthorhombic Forms of $Zn(Ph\text{-}S)_2(2,9\text{-}Me_2phen)$

	monoclinic	orthorhombic
Zn-S(1)	2.255 (2)	2.257 (4)
Zn-S(2)	2.255 (2)	2.270 (3)
Zn-N(1)	2.086 (4)	2.128 (7)
Zn-N(2)	2.086 (4)	2.114 (7)
S(1)-C(1)	1.758 (4)	1.768 (10)
S(2)-C(7)	1.758 (4)	1.777 (10)
N(1)-C(13)	1.340 (6)	1.341 (14)
N(1)-C(24)	1.346 (6)	1.371 (11)
N(2)-C(22)	1.340 (6)	1.327 (12)
N(2)-C(23)	1.346 (6)	1.361 (13)
C(1)-C(2)	1.391 (7)	1.362 (15)
C(1)-C(6)	1.388 (7)	1.398 (15)
C(2)-C(3)	1.386 (7)	1.395 (16)
C(3)-C(4)	1.368 (8)	1.356 (16)
C(4)-C(5)	1.374 (9)	1.358 (16)
C(5)-C(6)	1.392 (8)	1.396 (14)
C(7)-C(8)	1.391 (7)	1.395 (14)
C(7)-C(12)	1.388 (7)	1.381 (14)
C(8)-C(9)	1.386 (7)	1.383 (15)
C(9)-C(10)	1.368 (8)	1.368 (15)
C(10)-C(11)	1.374 (9)	1.384 (14)
C(11)-C(12)	1.392 (8)	1.379 (13)
C(13)-C(14)	1.391 (12)	1.400 (15)
C(13)-C(25)	1.461 (10)	1.478 (15)
C(14)-C(15)	1.368 (14)	1.330 (14)
C(15)-C(16)	1.383 (13)	1.401 (14)
C(16)-C(17)	1.423 (10)	1.433 (14)
C(16)-C(24)	1.411 (8)	1.402 (13)
C(17)-C(18)	1.281 (22)	1.367 (16)
C(18)-C(19)	1.423 (10)	1.418 (15)
C(19)-C(20)	1.383 (13)	1.383 (14)
C(19)-C(23)	1.411 (8)	1.425 (14)
C(20)-C(21)	1.368 (14)	1.356 (15)
C(21)-C(22)	1.391 (12)	1.396 (15)
C(22)-C(26)	1.461 (10)	1.511 (14)
C(23)-C(24)	1.443 (9)	1.430 (13)

Table S-III. Bond Angles (deg) for the Monoclinic and Orthorhombic Forms of $Zn(Ph\text{-}S)_2(2,9\text{-}Me_2phen)$

	monoclinic	orthorhombic
S(1)-Zn-S(2)	134.5 (1)	138.1 (1)
S(1)-Zn-N(1)	106.7 (2)	106.2 (2)
S(2)-Zn-N(1)	107.7 (1)	103.9 (2)
S(1)-Zn-N(2)	107.7 (1)	105.3 (2)
S(2)-Zn-N(2)	106.7 (1)	108.6 (2)
N(1)-Zn-N(2)	80.2 (2)	79.0 (3)
Zn-S(1)-C(1)	109.8 (2)	110.4 (4)
Zn-S(2)-C(7)	109.8 (2)	111.9 (3)
Zn-N(1)-C(13)	127.5 (4)	128.3 (6)
Zn-N(1)-C(24)	112.4 (3)	112.2 (6)
C(13)-N(1)-C(24)	120.0 (4)	119.5 (8)
Zn-N(2)-C(22)	127.5 (4)	127.6 (6)
Zn-N(2)-C(23)	112.4 (3)	113.4 (6)
C(22)-N(2)-C(23)	120.0 (4)	119.0 (8)
S(1)-C(1)-C(2)	124.5 (4)	120.6 (8)
S(1)-C(1)-C(6)	117.5 (4)	121.1 (8)
C(2)-C(1)-C(6)	118.0 (4)	118.1 (9)
C(1)-C(2)-C(3)	120.8 (5)	121.1 (10)
C(2)-C(3)-C(4)	120.9 (5)	120.2 (11)
C(3)-C(4)-C(5)	118.9 (5)	120.4 (11)
C(4)-C(5)-C(6)	121.1 (5)	119.9 (10)
C(1)-C(6)-C(5)	120.3 (5)	120.3 (10)
S(2)-C(7)-C(8)	124.5 (4)	117.9 (7)
S(2)-C(7)-C(12)	117.5 (4)	124.3 (7)
C(8)-C(7)-C(12)	118.0 (4)	117.8 (9)
C(7)-C(8)-C(9)	120.8 (5)	119.2 (10)
C(8)-C(9)-C(10)	120.9 (5)	121.8 (10)
C(9)-C(10)-C(11)	118.9 (5)	120.1 (10)
C(10)-C(11)-C(12)	121.1 (5)	117.8 (10)
C(7)-C(12)-C(11)	120.3 (5)	123.3 (9)
N(1)-C(13)-C(14)	119.4 (6)	119.5 (9)
N(1)-C(13)-C(25)	117.3 (5)	115.7 (9)
N(1)-C(24)-C(16)	123.6 (5)	122.7 (8)
N(1)-C(24)-C(23)	117.5 (2)	118.0 (8)
N(2)-C(22)-C(21)	119.4 (6)	122.1 (9)
N(2)-C(22)-C(26)	117.3 (5)	117.6 (8)
N(2)-C(23)-C(19)	123.6 (5)	121.4 (8)
N(2)-C(23)-C(24)	117.5 (2)	117.4 (9)
C(14)-C(13)-C(25)	123.3 (6)	124.8 (10)
C(13)-C(14)-C(15)	120.3 (7)	121.3 (9)
C(14)-C(15)-C(16)	121.7 (8)	121.4 (9)
C(15)-C(16)-C(17)	126.4 (7)	124.1 (9)
C(15)-C(16)-C(24)	114.9 (6)	115.6 (9)
C(17)-C(16)-C(24)	118.7 (7)	120.2 (9)
C(16)-C(17)-C(18)	122.3 (5)	118.6 (9)
C(16)-C(24)-C(23)	118.9 (4)	119.3 (9)
C(17)-C(18)-C(19)	122.3 (5)	124.4 (10)
C(18)-C(19)-C(20)	126.4 (7)	126.4 (10)
C(18)-C(19)-C(23)	118.7 (7)	116.2 (9)
C(20)-C(19)-C(23)	114.9 (6)	117.4 (9)
C(19)-C(20)-C(21)	121.7 (8)	120.4 (9)
C(19)-C(23)-C(24)	118.9 (4)	121.2 (9)
C(20)-C(21)-C(22)	120.3 (7)	119.7 (10)
C(21)-C(22)-C(26)	123.3 (6)	120.3 (9)

Table S-IV. Anisotropic Thermal Parameters ($Å^2 \times 10^3$)[a] for the Monoclinic and Orthorhombic Forms of $Zn(Ph\text{-}S)_2(2,9\text{-}Me_2phen)$

monoclinic						
Zn	60 (1)	38 (1)	52 (1)	0	20 (1)	0
S(1), S(2)	98 (1)	53 (1)	96 (1)	8 (1)	60 (1)	6 (1)
N(1), N(2)	46 (2)	61 (2)	60 (2)	21 (2)	18 (2)	4 (2)
C(1), C(7)	61 (3)	49 (3)	62 (3)	-7 (2)	19 (2)	1 (2)
C(2), C(8)	79 (4)	58 (3)	80 (3)	-2 (3)	35 (3)	0 (3)
C(3), C(9)	77 (4)	59 (3)	77 (4)	9 (3)	12 (3)	-9 (3)
C(4), C(10)	72 (4)	58 (3)	99 (4)	-5 (3)	4 (3)	5 (3)
C(5), C(11)	66 (4)	78 (4)	96 (4)	-21 (3)	14 (3)	12 (3)
C(6), C(12)	64 (3)	73 (4)	62 (3)	-14 (3)	20 (3)	6 (3)
C(13), C(22)	50 (3)	132 (5)	63 (3)	38 (4)	23 (3)	10 (3)
C(14), C(21)	60 (4)	210 (9)	106 (6)	90 (7)	33 (4)	44 (6)
C(15), C(20)	89 (6)	155 (8)	189 (10)	123 (8)	85 (7)	71 (6)
C(16), C(19)	83 (5)	68 (4)	179 (7)	55 (5)	83 (5)	31 (4)
C(17), C(18)	131 (12)	42 (3)	335 (23)	41 (6)	154 (12)	23 (4)
C(23), C(24)	51 (3)	49 (3)	110 (4)	23 (3)	50 (3)	11 (2)
C(25), C(26)	87 (5)	184 (8)	61 (3)	-9 (4)	3 (3)	-33 (5)
orthorhombic						
Zn	45 (1)	33 (1)	55 (1)	-1 (1)	-2 (1)	-1 (1)
S(1)	83 (2)	42 (2)	137 (4)	11 (2)	-62 (2)	-9 (2)
S(2)	68 (2)	44 (2)	72 (2)	-14 (2)	-25 (2)	14 (2)
N(1)	42 (5)	34 (5)	41 (6)	10 (5)	-2 (5)	4 (4)
N(2)	19 (5)	51 (6)	37 (6)	5 (5)	-1 (4)	-6 (4)
C(15)	52 (7)	55 (7)	47 (9)	-21 (6)	-25 (6)	16 (6)
C(17)	82 (10)	30 (6)	75 (11)	-8 (7)	-23 (9)	17 (7)
C(18)	72 (9)	39 (7)	93 (12)	5 (8)	-5 (9)	-5 (7)
C(20)	45 (7)	63 (8)	66 (9)	30 (7)	-7 (7)	-24 (6)
C(25)	65 (8)	100 (11)	69 (10)	26 (9)	20 (8)	15 (8)
C(26)	47 (7)	90 (10)	65 (9)	-18 (9)	5 (7)	14 (8)

[a] The anisotropic temperature factor exponent takes the form: $-2\pi^2(h^2a^* {}^2U_{11} + \cdots + 2hka^* b^* U_{12})$.

Table S-V. Hydrogen Atom Positions (x 10^4) and Isotropic Thermal Parameters ($Å^2$ x 10^3) for the Monoclinic and Orthorhombic Forms of Zn(Ph-S)2(2,9-Me2phen)

	monoclinic				orthorhombic			
	x	*y*	*z*	*U*	*x*	*y*	*z*	*U*
H(2)	626	691	3586	83	2239	6658	3099	67
H(3)	1020	-951	4254	88	2268	8335	3230	70
H(4)	2006	-1906	3412	93	1945	9106	4752	85
H(5)	2628	-1191	1917	96	1606	8227	6180	81
H(6)	2217	439	1195	81	1604	6539	6102	78
H(8)[a]					277	6647	1052	61
H(9)[a]					150	8295	1252	79
H(10)[a]					430	9114	2786	68
H(11)[a]					809	8269	4239	69
H(12)[a]					945	6630	4029	61
H(14)[a]					2167	2424	653	67
H(15)[a]					1927	1033	1464	61
H(17)[a]					1443	159	2980	69
H(18)	-478	7228	1650	177	939	300	4495	69
H(20)	-1738	4654	-992	146	510	1345	5944	71
H(21)	-1296	6213	-151	156	333	2874	6571	61
H(25A)[a]					2089	4197	546	84
H(25B)[a]					2280	4482	1719	84
H(25C)[a]					1745	4750	1363	84
H(26A)	1745	4750	1363	84	295	4619	6184	77
H(26B)	2280	4482	1719	84	577	5093	5200	77
H(26C)	2089	4197	546	84	869	4656	6193	77

[a] Atoms generated by an inversion symmetry operation.

DL/1113/89/1

TECHNICAL REPORT DISTRIBUTION LIST, GENERAL

	No. Copies
Office of Naval Research Chemistry Division, Code 1113 800 North Quincy Street Arlington, VA 22217-5000	3
Commanding Officer Naval Weapons Support Center Attn: Dr. Bernard E. Douda Crane, IN 47522-5050	1
Dr. Richard W. Drisko Naval Civil Engineering Laboratory Code L52 Port Hueneme, California 93043	1
Defense Technical Information Center Building 5, Cameron Station Alexandria, Virginia 22314	2 high quality
David Taylor Research Center Dr. Eugene C. Fischer Annapolis, MD 21402-5067	1
Dr. James S. Murday Chemistry Division, Code 6100 Naval Research Laboratory Washington, D.C. 20375-5000	1
Dr. Ronald L. Atkins Chemistry Division (Code 385) Naval Weapons Center China Lake, CA 93555-6001	1
Chief of Naval Research Special Assistant for Marine Corps Matters Code 00MC 800 North Quincy Street Arlington, VA 22217-5000	1
Dr. Bernadette Eichinger Naval Ship Systems Engineering Station Code 053 Philadelphia Naval Base Philadelphia, PA 19112	1
Dr. Sachio Yamamoto Naval Ocean Systems Center Code 52 San Diego, CA 92152-5000	1
David Taylor Research Center Dr. Harold H. Singerman Annapolis, MD 21402-5067 ATTN: Code 283	1